DEVELOPED CYCLIC PLATE LOAD TEST FOR GEOSYNTHETICS-REINFORCED UNPAVED ROAD OVER SOFT SUBGRADE

Nicole KHOUEIRY [a]- PhD Student, GEOMAS

Laurent BRIANCON [a] - Assistant Professor, GEOMAS

Mathilde RIOT [b] - R&D and technical director, AFITEXINOV

Ali DAOUADJI [a] - Professor, GEOMAS

[a] *Université de Lyon, INSA-Lyon, GEOMAS, 34 Avenue des Arts 69621 Villeurbanne Cedex, France*

Phone: +33 472 438 370

E.mail: Nicole.khoueity@insa-lyon.fr

E-mail: Laurent.briancon@insa-lyon.fr

Email: Ali.daouadji@insa-lyon.fr

[b] *AFITEXINOV, 56 Route de Ferrossière, 38110 Saint-Didier-de-la-Tour, France*

Phone: +33 437 050 879

Email: mathilde.riot@afitex.com

ABSTRACT

With the expansion of urban areas, the construction on soft subgrade becomes a more often issue due to excessive settlement, especially for roads network. Nowadays, the tradition soft soil replacement solution is substituted by stabilization solutions to reduce the surface settlement. Geosynthetics (GSYs) are used to stabilize base course over soft subgrade under unpaved roads. GSYs improve this structure by the following mechanisms: lateral restraint and reinforcement of base course aggregates, tension membrane effect in rutted areas, and reduction of mixing between subgrade and base soils. With the reinforcement addition, the mechanisms developed at the interface become even more complex. It is important to identify and clarify these mechanisms in order to propose an efficient design method for this kind of structure.

A large-scale laboratory test was designed and developed to characterize the GSYs effects and the reinforcement mechanisms in unpaved roads. An unpaved road platform was subjected to cyclic plate load. The platform consisted of a soft subgrade layer supporting a base course layer and placed in a box of 1.9 m of large, 1.8 m of length and 1.1 m of height. The composition of soft soil, the installation and the quality control procedure are detailed in this paper. The surface rutting, the subgrade settlement and the vertical stress distribution were monitored during the loading cycles. Moreover, the GSY strain was monitored using the fibre optic technology.

Six tests were performed; two repeatability tests and four reinforced and unreinforced tests with different base course thicknesses. The tests performed proved the repeatability of the experimental protocol. Moreover, it is concluded that the used GSY has a negligible effect if the base course thickness is equal or higher than 350 mm. On the other hand, for a base course thickness of 220 mm, the geogrid reinforcement provides a surface rutting reduction of 22%, and a subgrade central vertical stress reduction of 30%. In comparison with the empirical and the analytical design methods from the literature, we conclude that these methods overestimate

the base course thickness for unreinforced platform. These experiments consist in a preparation program to a full-scale experiment, with a cyclic Traffic load applied on the unpaved road surface, using the Simulator Accelerator of Traffic (SAT) machine developed at INSA Lyon.

Keywords: Geosynthetic, soft subgrade, unpaved roads, cyclic load

1. INTRODUCTION

In the last few decades, geosynthetics (GSYs) were widely used in Civil engineering and especially in geotechnical field. In fact, GSYs can provide seven different functions as separation, drainage, filtration, protection, watertighness, erosion protection and reinforcement. Due to their high mechanical properties, the GSYs are used for soil reinforcement in geotechnical constructions: retaining walls, pile supported embankments, sinkholes, unpaved roads and soft subgrade, etc…

Since 1970, the GSYs were used extensively in base course reinforcement (unpaved road and areas). Actually, it is an economic alternative solution comparing to the soil replacement. Indeed, the GSY reinforcement allows the base course thickness reduction. In these structures, the reinforcement can be placed at the interface between the soft soil and the base course layer or in the base course layer in order to reinforce it and reduce the rutting development at the road surface.

The complex reinforcement phenomenon in this platform depend on various mechanisms as:

- The lateral restraint mechanism: By adding a tension stiffness at the bottom of the base course, the lateral movement of the aggregates under the wheels load is blocked. This mechanism reduces the shear stress on the subgrade top and increases the stiffness of the base course layer. Consequently, the vertical stress on the surface of the subgrade decreases. In fact, this is a two-layer system, and the stress distribution on the lower layer depends on the relative modulus of the two layers.

  It is important to note that the GSY adds the tension stiffness to the base course by two mechanisms: interface friction between GSY and aggregates and, when a geogrid is used, interlocking between GSY and aggregates.

  Based on previous studies, the confining mechanism does not imply important surface rutting.

- The separation mechanism: This mechanism is important to conserve the well-compacted base course layer properties. In fact, the separation prevent the loss of aggregates particles in the soft soil and the incorporation of the fine materials into the base course layer. Geotextiles are typically used to provide the separation function. However, Giroud (2009) mentioned that a geogrid with appropriate aperture size can also provide the separation function.
- The tension membrane effect: the tension developed in a curved GSY results in an upward force supporting the wheel load. The effect of this mechanism increases with the increasing of the rutting form (Perkins and Ismeik, 1997). In the early studies on the GSY reinforcement mechanisms in such application, the membrane effect was the dominant mechanism. However, recent works have shown that this is not the case (Giroud, 2009).

As mentioned previously the mechanisms developed on the GSY interface are complex and depend on various factors. In addition, there is still a misunderstanding regarding the mechanism that governs the unpaved road behaviour. More experimental studies and research works are required to provide more knowledge and clarify these mechanisms.

The aim of the present work is the development of a cyclic plate load test on an unpaved road. This testing facility will be used to compare the benefits of different GSY manufacturing types, the improvement of the existing analytical design methods and the development of numerical design methods. The subgrade and the base course constitution, preparation and installation procedures are particularly detailed. Moreover, the repeatability testing of this experimental protocol and the results obtained are given in this paper.

2. BACKGROUND

2.1. Experimental tests

The performance of the GSY in the reinforcement of unpaved roads on soft subgrade depends on the base course properties and thickness, the subgrade properties, the GSY position and number of layers, the GSY tension stiffness. Moreover, the aggregates-geogrid interlocking effect depends on the geogrid aperture size compared to the aggregates size, the geogrid aperture shape, the shape and stiffness of ribs and the stiffness of junction between ribs (Hufenus et al., 2006; Giroud, 2009; Qian et al., 2013).

The complexity of the mechanisms that govern the performance of the unpaved reinforced roads resulted in a wide research works. In fact, two laboratory test approaches have been used in the literature to evaluate the performance of the reinforcement: the monotonic plate loading and the cyclic plate loading.

Dong et al. (2010) performed a static laboratory plate load test, and compared the ratio of bearing capacity of each test in order to study the influence of the changed factors: the aperture shape, the geogrid location and the number of geogrid layers. Based on their results , the authors concluded that the geogrid placed at the depth of 2/3 of the plate diameter performed better than other positions.

Another static plate load test was performed by Abu-Farsakh et al. (2016) in the aim of evaluating the effect of the GSY type, the GSY location, the number of GSY layers, and the tensile modulii. Abu-Farsakh et al. (2016) performed 22 different tests, and based on the comparison of the bearing capacity ratio between these tests, they concluded that the double reinforcement location contributes to the best platform improvement.

A comparison between a monotonic plate loading and cyclic plate loading was performed by Palmeira and Antunes (2010), and the results showed that the tests under monotonic loading conditions underestimate the benefits of the reinforcement. On the other hand, Palmeira and

Antunes (2010) compared the effect of the two GSY types (a geogrid and a woven geotextile) under cyclic plate load test of 566 kPa and 1 Hz of frequency, and concluded that the geogrids provided a better overall performance than geotextiles in this application due to the interlocking effect. This study addressed the performance of these reinforced platforms after maintenance of the surface.

The large geotechnical test box (2 x 2.2 x 2 m) developed at the University of Kansas was also used to perform various cyclic plate load tests at frequency of 0.77 Hz. Qian et al. (2011) used this apparatus to perform cyclic plate load tests and compared the effect of geogrid aperture shape. The experimental study showed that a triangular aperture shape performed better than a rectangular shape. Qian et al. (2013) used the same device to compare this time the effect of base course thickness. Three different thicknesses were tested (150 mm, 230 mm and 300 mm). The experimental results showed the effect of the reinforcement on the reduction of the maximum vertical stress on the subgrade surface for the three different base coarse thicknesses. Moreover, the authors concluded that the more robust and thicker the GSY is the more important is the benefit in the platform behaviour improvement.

Sun et al. (2015) performed the same test procedure to investigate the effect of load intensity on pavement response. In this test, every 100 cycles, the load intensity was increased from 5 kN to 50 kN.

The quality control procedure was the same in these three studies. It is important to note that the geogrids tested in these studies had the same manufacturing type.

More recently, Satyal et al. (2018) used this device to test the performance of geocell in improving the railways on soft subgrade. In fact, the soft soil part remained the same, and this time it was covered with 300 mm of a ballast layer reinforced by geocell. The platform was subjected to 6,000 cycles, the load amplitude increased every 1,000 cycles, starting from 10 kN and reaching 60 kN. The results showed that the geocell reinforcement decreases the surface settlement and the applied vertical stress on the subgrade surface.

Kim et al. (2006) conducted cyclic plate load tests on a reinforced and unreinforced platforms. Four different GSY types and two different base course thicknesses were tested. Based on the results, the authors observed a linear relation between the thickness ratio (which is the ratio of the required thickness to achieve a target deflection for a given base course type (h) and the required thickness to achieve the same deflection for a breaker run stone (h_{br})) and the GSY-Base course interaction modulus, obtained from a pull-out test.

Christopher and Perkins (2008) performed a cyclic plate load test regarding the AASHTO 4E-SR method to evaluate the GSY drainage function in this application. The authors concluded that the non-woven geotextile due to its drainage capacity could reduce the pore pressure in the subgrade. Moreover, they stated that the rutting is highly related to the pore pressure development in the subgrade.

Moreover, Gabr (2001) performed a cyclic plate load test, and illustrated the variation of the load distribution angle of the base course with the number of cycles. And based on the results of his study two analytical methods were developed to design the reinforced unpaved roads (Giroud and Han, 2004; Leng and Gabr, 2006).

In order to understand the reinforcement mechanism in these structures other authors performed full-scale tests with a cyclic wheel load. Hufenus et al. (2006), Cuelho and Perkins (2009a) and Cuelho et al. (2014) performed in situ tests on an unpaved road with various GSY types, in order to compare the bearing capacity and serviceability of the platforms. In these tests, trucks were used to apply the loading cycles.

The preparation of these tests takes time, and the results can be affected by the weather conditions and the non-homogeneity of the subgrade. Moreover, since the load application is not automatic the loading cycle number is limited.

Watts et al. (2004), Jersey et al. (2012), Norwood and Tingle (2014), Yang et al. (2012) and Cook et al. (2016) performed a large-scale laboratory test with a cyclic wheel load using the Accelerated Pavement Testing (APT) facilities to reduce the test variability and external influences. This indoor test facility allows the control of the load cycles magnitude, velocity and the soils parameters. However, these tests still need long preparation regarding the platform dimensions. Therefore, it is interesting to develop a full-scale test with automatic cyclic load application, and optimise the platform dimensions to reduce the test preparation time. For this reason, a Simulator Accelerator of Traffic (SAT) was developed and appropriated for this application.

The work presented in this paper aimed to prepare and approve the experimental protocol before passing to the tests using the SAT machine. In the literature little information were provided regarding the soft soil preparation and control. However, in this work a special attention was given to the soil preparation and quality control in order to have a repeatable test protocol. Moreover, in the literature the tests were limited regarding the number of cycles applied at the surface. In this study, 10,000 cycles were applied on the surface even if 75 mm of surface deformation was reached.

2.2. Design methods

Since 1970, various empirical design methods and analytical methods have been developed in order to determine the base course thickness by considering the GSY effect.

Based on a large testing program proposed by US Corps and Engineer, Hammitt and Iii (1970) proposed an empirical design method for unreinforced unpaved road. This method consists of calculating the aggregate thickness for a rutting criterion of 75 mm. Giroud and Noiray (1981) proposed another empirical formula for unreinforced unpaved road with other rutting criteria. Moreover, Giroud and Noiray (1981) proposed a theoretical design method for reinforced unpaved roads based on the large displacement mechanism. This design method was further elaborated by Giroud (1984). The reinforcement was included in the equations as a stress distribution improvement and a normal stress difference due to the tension membrane effect.

Milligan et al. (1989) developed an analytical design method based on the small displacement mechanism of reinforced unpaved road. This method allows the calculation of the tension developed in the GSY based on the stress analysis at the base and subgrade shear interface.

More recent researches has been carried in this field and more analytical methods were developed (Giroud and Han, 2004; Leng and Gabr, 2006). In fact, Giroud and Han (2004) improved the methods developed earlier to determine the base course thickness of unreinforced and GSY-reinforced unpaved roads. This design method was developed for geogrid-reinforced unpaved road, and takes the interlocking between the aggregates and the geogrid into account, the in-plane aperture stability modulus of the geogrid and stress distribution angle degradation with cycles. This design method has been included in the “GSY Design and Construction Guidelines” manual by the FHWA (2008).

Leng and Gabr (2006) provided a further development in the geogrid-reinforcement unpaved roads design. This method is based on Odemark’s method, which is an approximate method to transform a two-layer system with different modulus in an equivalent one-layer system. This method takes the stress distribution angle, the base course and the subgrade moduli degradation with cycles into account.

It is important to note that both methods (Giroud and Han, 2004; Leng and Gabr, 2006) were calibrated based on laboratory tests (Gabr, 2001), and these tests were performed on one specific GSY manufacturing type. Indeed, the existing design methods were calibrated and based on specific cases and configurations.

The aim of this work is to compare the experimental results with the existing design methods in order to verify the reliability of these methods.

3. EXPERIMENTAL DEVICE

The tested platform was placed in a box of 1.9 m of large, 1.8 m of length and 1.1 m of height. The borders of the box were covered with plastic films to prevent the water content variation. At the bottom of the box 200 mm of well-compacted aggregates were placed and covered with anti-vibration mat to limit the vibration propagation.

The test consisted of applying a cyclic load using a 300 mm diameter plate on the surface of an unpaved road supported by a soft subgrade. The maximum load applied to the surface of the platform was 40 kN, which is equal to the a half-axle load (ESAL : Equivalent Single Axle Loads) based on the American standard AASHTO (1993) with an applied pressure of 566 kPa. The cycle load waves were generated by a hydraulic loading system (Figure 1). The maximum load was maintained for 0.2 second, the unload phase was maintained for 0.5 sec, and the loading-unloading phase was done in 0.6 sec.

The unpaved road tested with this facility were subjected to 10,000 cycles, with a maximum rutting of 75 mm regarding the FHWA (2008) standard.

The granular platform was supported by 600 mm of artificial unsaturated soft subgrade. The CBR of the soft subgrade should be less than 3 % so a GSY reinforcement is in need regarding the FHWA (2008) standard. The soft soil composition, installation and quality control are presented in the next sections. The CBR required for the granular platform is 20 % (FHWA, 2008). Two granular platform thicknesses were tested, 350 mm and 220 mm.

4. TESTS

As mentioned in the previous Section, this experimental protocol was developed in order to compare the effect of different GSY. In this paper, the results of six tests are presented (Table 4):

- Two tests with a base course thickness of 350 mm, with and without reinforcement,
- Two repeatability tests with a base thickness of 220 mm, with reinforcement,

- Two identical tests without any reinforcement and with 220 mm of base course thickness.

5. MATERIALS

The tested platform consisted of 600 mm of soft subgrade and a variable base course thickness. In order to simulate a soft subgrade in the laboratory and to reconstitute for every test the same subgrade properties, a well-calibrated artificial subgrade was used.

5.1. Soft subgrade constitution

Regarding the FHWA (2008) Standard, a base course reinforcement is necessary when the CBR ratio of the subgrade layer is less than 3 %, noting that the CBR ratio is determined regarding the ASTM-D4429 Standard.

In order to simulate the same subgrade with the same properties for every laboratory test an artificial subgrade was constituted of a clay and sand mixture.

Different mixtures were tested to get the mixture constitution that will reach a CBR ratio of 2% at the right side of the proctor optimum, within an unsaturated situation.

Two clay types were tested: the calcium bentonite and the kaolinite. The Hostun sand (HN 34) was used in all the mixtures. For each clay type, four different percentages were tested: M1 (20 % Clay, 80 % Sand), M2 (25 % Clay, 75 % Sand), M3 (30 % Clay, 70 % of Sand), M4 (40 % Clay, 60 % of Sand).

The particle size distribution was drawn for each mixture to verify that the two materials can be well Mixed (Figure 2).

For all the mixture combinations, the Proctor and CBR curves were drawn. Based on these curves, the water content over which the mixture was compacted to get a CBR of 2 % was determined (Figure 3).

The results show that when the percentage of clay increases in the mixture the percentage of saturation at the point giving a CBR of 2 % increases (Table 1).

In this test protocol, an unsaturated subgrade is considered. For this reason, the M1 (20 % Clay, 80 % Sand) mixture with the Kaolinite Clay has been chosen. Indeed, the degree of saturation of this mixture at the point giving a CBR of 2 % is 75 %.

5.2. Aggregates

The aggregates used in these tests are non-treated aggregates with particles diameters ranging between 0 and 31.5 mm (GNT 0/31.5), which is the most commonly used material in France for road constructions.

Figure 4 illustrates the aggregates size distribution. Based on the curve the Cu and Cc factors are respectively equal 20 and 5. This soil is classified as a GP (poorly graded gravel) soil regarding the USCS standard and D_2 regarding the GTR standard.

The CBR required for the base course layer is 20 % regarding the FHWA (2008) standard. Figure 5 illustrates the proctor and CBR curves of the aggregates. Since the plate vibrator used to compact this layer is not qualified for the compaction of this material, we will test in the large scale the compaction of the aggregates at 4% of water content and fix the compaction protocol that will give us the 20% of CBR.

5.3. GSYs

A layer of a thin non-woven geotextile (17 g/m^2) was placed under the geogrid layer in order to separate the soils layers. The GSY used in this test is a knitted and coated geogrid (Table 2). This product has a special manufacturing process. In fact, the yarns are joined with a special knitting technology that keeps the yarns in a straight position. This straight yarns initial position allows the development of tension in the product after a relatively small deformation, which is not the case when the initial manufacturing yarns state presents curves (Figure 6). The product apertures have a square shape, with a dimension of 40 mm. The maximum tension strength is equal in both directions (Table 2). More importantly, the manufacturing technology allows the implementation of fibre optics in the product yarns during the production.

6. INSTRUMENTATION

The aim of this test is to improve the knowledge regarding the mechanisms developed at the base coarse and soft subgrade interface with geosyntheic reinforcement. To reach this goal, the test was instrumented with Earth Pressure Cells (EPC), settlement sensors (S) and displacement sensor (Table 3). Inclinometers were placed on the earth pressure cells, in order to monitor the horizontality of the sensors during the test.

In order to monitor the vertical stress distribution on the subgrade surface, five earth pressure cells were placed in five different positions from the plate load centre (Figure 6). Moreover, earth pressure cells were placed in different depth positions under the plate centre. In addition, five settlement sensors were placed in different positions at the subgrade surface to monitor the vertical surface displacement occurring during cycles. This settlement sensors were interconnected by means of a pressure line, an air compensation line and a digital data cable. The sensor elevation changes is measured in terms of liquid pressure variation.

Two kind of data acquisition logger were used: Data Taker data logger, Scaime measurements acquisition instrument. The data taker logger was used to take static measurements between each loading series. In fact, the limitation of this logger is the measurement of continues values with high frequency. The settlement sensors and some earth pressure cells were connected to this logger. In addition, the scaime measurements acquisition instrument was used for continuous measurements during cycles. In fact, the advantage of this data logger is that it aliments the all channels at the same time and it can read continuous output values. The used sensors connected to this logger are the earth pressure cells placed at the subgrade surface, the laser sensor and the inclination sensors.

A load cell was placed on the plate to monitor and control the load magnitude. In addition, a displacement laser sensor was used to monitor the plate displacement during the test, and to draw the settlement curve at the platform surface after the 10,000 cycles. Moreover, a fibre optic sensor was placed in the GSY in order to measure the deformation developed in the reinforcement during the loading. The spread sensor technology was used in this application. This technology is based on the Rayleigh backscattering phenomenon thanks to an interferometric optical assembly based on Optical Frequency Domain Reflectometry (OFDR). These interrogators allow distributed measurements of deformation and temperature along a single optical fibre. This measurement method results in thousands of measurement points, at centimetre or even millimetre spatial resolution, over very long lengths up to 50 m.

7. TEST SETUP

7.1. Soft soil

A grout mixer was used to mix the 80 % of Hostun sand and the 20 % of kaolinite at a targeted water content of 11.5 %. In addition, a vibrator plate compactor was used to compact the layers and get the desired dry density of 18.8 kN/m^3.

Several installation protocols were tested in order to establish the protocol that will give a homogenous soil over the layers with a CBR of 2 %. For each protocol, different tests were performed to control the homogeneity and the CBR all over the layer.

The relevant protocol used for subgrade installation consisted of placing:

- The first 200 mm are placed without any compaction, since this layer will be subjected to the compaction of the above layers.
- The next 200 mm are compacted with one compactor pass by layers of 100 mm.
- A layer of 100 mm is compacted with one compactor pass.
- The last 100 mm of soil is not subjected to any compaction, since this layer will undergo the compaction of the gravel layer.

7.2. Aggregates

It is important to note that in the large-scale compaction over the soft soil the maximum proctor and the CBR of 20 % could not be reached. Many installation protocols were tested for this layer too. The installation protocol adopted gives a dry density of 21.5 kN/m^3 and a CBR ranging between 10% and 15 %. This protocol consisted of placing two layers of 110 mm and compact each layer with four compactor passes.

8. QUALITY CONTROL TESTS

In order to compare the effect of GSY reinforcement in this test, variability of the soils properties is not allowed. Therefore, a series of quality control tests were performed on each soil layer prepared for testing. The quality control tests consist of a water content profile, a static and a dynamic penetrometer tests.

The water content profiles along the subgrade depth were plotted before and after each test to make sure that the subgrade water content does not change during the test. The results show that the subgrade water content remains constant during the test (Figure 8). Moreover, the initial water content before each test is +the same and homogeneous all over the surface and the depth.

The static penetrometer test was performed in the subgrade using the CBR cone, and the results were correlated to the CBR value. Moreover, the dynamic penetrometer test was performed in the subgrade and the base course layer, and the results were as far as correlated to the CBR value using Kleyn and Van Heerden formula given by the manufacturer technical file:

$$\mathrm{Log}_{10}\,(\mathrm{CBR}) = 2.632 - 1.28\,\mathrm{Log}_{10}\,(\mathrm{DCP}) \qquad \textit{Eq.1}$$

Where DCP is the depression per blow (mm/blow).

By comparing the results of the static and the dynamic penetrometer in the subgrade layer, we obtain the same CBR correlated value, which confirmed the correlation reliability.

The dynamic penetrometer results show the CBR profile in depth plotted for the soil layers prepared before every test (Figure 9). The graphs superposition confirms the soil repeatability for different tests. In fact, the soil installation protocol mentioned above resulted in the composition of a homogeneous and repeatable soil layers allowing the results comparison between a test and another.

Moreover, it is shown in the graphs (Figure 9) that the base course CBR values for 100 mm from the surface are around 5 %, this is due to the soil repulsion on the surface. However, more in the depth the CBR varies between 10 and 15 %, it reach 20% in some points. More in depth the subgrade CBR values is constant and around 2%.

9. RESULTS AND ANALYSIS

During these tests, the subgrade surface displacement, the base course surface displacement and the stress distribution were monitored. The platforms were subjected to 10,000 cycles, and the maximum rutting criteria used in the work is 75 mm regarding the FHWA (2008) standard. The rut development at the platform surface is an important criterion in the results analysis, since it is the base of the design process. There are two rutting definition, the 'elevation rut' and the 'apparent rut' (Cuelho and Perkins, 2009b). The rut depth was measured using a laser sensor, and the rut was the difference in the elevation of the measurement points over time witch is referred to the 'elevation rut' (Figure 10).

9.1. Repeatability tests

Two repeatability tests were performed on a reinforced and unreinforced platform with the thickness H = 220 mm. The maximum rut for the reinforced identical tests is 69 mm and 61 mm (tests 5 and 6) after 10,000 cycles (Figure 11). The maximum rut value after 10,000 cycles for the identical unreinforced tests is 90 mm and 97 mm (tests 3 and 4) (Figure 11).

Moreover, Figure 12 shows that the maximum subgrade surface settlement after 10,000 cycles for the reinforced identical tests is 63 mm and 61 mm (tests 5 and 6) and 82 mm and 78 mm for the unreinforced identical tests (tests 3 and 4). A difference of 8 mm regarding the allowable rutting displacement of 75 mm can be considered as a negligible variation. The close results given by the identical performed tests are more obvious in Figure 13. Indeed, the two identical performed tests give the same settlement evolution curves. These identical profile shapes and values given for the identical repeatability performed tests in both reinforced and unreinforced cases prove a good repeatability of the test and the installation protocol. It is important pointing out the symmetric settlement profile shape shown in Figure 11. This explains the instrumentation of one-half of the platform.

9.2. Base course thickness influence

Two tests were performed with a base course thickness of 350 mm, one with reinforcement (test 2) and another without reinforcement (test 1). Figure 11 shows a small difference in final rutting for H = 350 mm between a reinforced and an unreinforced platform. In fact both curves for H = 350 mm have the same shape with an average maximum rut of 44 mm for the unreinforced platform and 50 mm for the reinforced platform. The results shows that the reinforcement effect can be negligible for a base course thickness of 350 mm. Moreover, this can be shown in the subgrade surface settlement Figure 12.

It is worth pointing out that the base course thickness has the most significant influence on the surface rut development. In fact, by comparing the two unreinforced tests for H=220 mm and for H=350 mm, an evident rut reduction is observed (Figure 11). For 130 mm of base course thickness variation, the surface rut pass from 44 mm to 89 mm.

9.3. GSY benefit

The maximum rut for the unreinforced platform is 90 mm and 69 mm for the reinforced platform (tests 3 and 5). The reinforcement reduced the surface rutting of 20 mm (22%). The same is shown in Figure 12, a reduction of the maximum settlement at the subgrade surface of 21 % after 500 cycles and 24 % after 10,000 cycles.

Regarding the settlement curve developed on the subgrade surface, it is shown in Figure 12 that at 400 mm and 600 mm from the plate centre at the subgrade surface the settlement is null for reinforced and unreinforced case.

In order to clarify the effect of reinforcement on the rut and settlement development, Figure 13 and Figure 14 show the evolution of the maximum settlement at the subgrade and the base course surface with cycles. Without reinforcement, the maximum allowable rutting of 75 mm is reached after 350 cycles, while with reinforcement this allowable rutting is reached after 8500 cycles. Both rutting evolution curves (Figure 14) show a linear evolution after 2,000 cycles. This linear part is characterised by a slope of 1.4% without reinforcement and 1% with reinforcement. In addition, the subgrade settlement curves (Figure 14) show a linear evolution after 2,000 cycles, and this part is characterised by a slope of 0.085% without reinforcement and 0.053% with reinforcement.

However, it is shown in the graph (Figure 14) that for the first cycle the difference in rut development between a reinforced and unreinforced platform is equal 9 mm, and after 10,000 cycles, this difference is equal 20 mm. It is then worth pointing out that the GSY, effect is more important more the settlement is important, and this is because of the tension developed in the GSY.

Moreover, Figure 13 and Figure 14 show a lag between the settlement developed on the base course layer and the settlement developed over the subgrade surface for both cases. This lag is due to the base course thickness reduction with the cycles. The evolution of the base course thickness reduction with cycles is shown in Figure 15. The graph (Figure 15) shows an influence of the reinforcement on the base course thickness reduction. In fact, with the reinforcement inclusion the base course thickness reduction decreases.

Figure 18 shows an important influence of the reinforcement on the maximum vertical stress at the subgrade centre either for the first cycles or for the further cycles. In fact, after 500 cycles, the maximum stress decreases from 290 kPa without reinforcement to 220 kPa with reinforcement (tests 3 and 5), and after 10,000 cycles the maximum stress decreases from 296 kPa without reinforcement to 246 kPa with reinforcement.

This stress reduction can be due to the increasing of the base course stress distribution angle or to the resultant of the tension membrane developed in the reinforcement. In fact, in Figure 16 the distribution stress curve seems to be the same for both reinforced and unreinforced cases, but the difference could occurs between 200 mm and 400 mm from the centre plate. Unfortunately, the rotation of the earth pressure cells between 200 mm and 400 mm reduces the accuracy of the results in this area.

Figure 17 shows the central stress profile variation with depth for different cycle's states. The position variation of the earth pressure cells with the soil settlement during cycles is taken into consideration in this graph. This graph (Figure 17) shows that at 600 mm in depth from the platform surface the central vertical stress is not affected by the reinforcement. On the other hand, at 400 mm in depth from the platform surface the central vertical stress decreases about 30 % with reinforcement. In addition, the central vertical stress at the subgrade/base course interface is subjected to a reduction of 17% with the reinforcement. Moreover, it is shown in the graph (Figure 16 & Figure 17) that the central vertical stress increases with cycles. This can be due to the base coarse layer degradation with cycles.

In order to highlight the reinforcement benefit the traffic benefit ratio (TBR) was calculated, at 45 mm, 60 mm and 75 mm of surface rutting:

$$TBR = \frac{\mathrm{N}_{reinforced}}{N_{unreinforced}} \qquad Eq.2$$

Where $N_{reinforced}$ is equal to the number of load cycles for the reinforced base at a certain permanent deformationand $N_{unreinforced}$ the number of load cycles for the unreinforced base at the same permanent deformation.

Table 5 presents the number of load cycles for the three different settlement values for the reinforced and the unreinforced platforms for the base course thickness of 220 mm and the TBE values. In fact, the reinforced platform reaches 45 mm of rutting after 100 cycle, while the unreinforced platform reaches this rutting after 50 cycles.

It is shown (Table 5) that the TBR increases depending on the allowable rutting criteria. In fact, for 45 mm, the TBR is equal 2 and for 75 mm the TBR is equal 24.3. We can state that the GSY benefit is more important for high allowable rutting criteria.

Moreover, Figure 18 illustrates the subgrade central vertical stress state for this same three rutting displacement. This graph (Figure 18) shows clearly the stress increasing for the reinforced platform with rutting development.

9.4. GSY strain

A fibre optic sensor was placed inside the GSY. Due to the OFDR technology, the continuous strain developed in the GSY was measured even during the cycles. Measurements were taken even after the base course installation. Figure 19 illustrates the developed strain in the GSY during the base course installation; it shows that the developed strain is in average equal to 1,500 με. From the strain, the tension developed in the GSY is calculated knowing that the product stiffness is equal 1,000 kN/m. The developed tension is equal 1.5 kN/m, which is 1.5% of the product ultimate tensile strength.

After the base course installation, the strains are put again to zero in order to measure the deformation due to the loading.

Moreover, Figure 20 shows the developed strain in the GSY after the application of 1,000 cycles, under applied load and during the unloading stage. The maximum strain reached at the centre during the loading is equal to 13,000 με, and during the unloading, is equal 8,000 με. This shows the elastic and the plastic deformation developed in the GSY during the loading and unloading. In fact, the plastic deformation is about 60% of the total deformation developed during the loading. Moreover, regarding the force developed in the GSY during the loading, it is equal 15% of the ultimate tension strength.

At a distance of 200 mm from the box edge, the deformation due to the loading is null. This shows that there is no Anchorage effect on the results and the GSY behaviour and that the developed tension in the GSY is taken by the interaction with the base course layer before it reaches the box edges.

10. EMPIRICAL AND ANALYTICAL DESIGN METHODS

The design methods proposed in the literature allow the aggregate thickness determination based on the rutting development, the cycle number, the subgrade and base course stiffnesses and the GSY reinforcement contribution.

Hammitt and Iii (1970) proposed the following empirical formula for unreinforced unpaved road with rutting criteria of 75mm:

$$H = (0.0236\log N + 0.0161)\sqrt{\frac{P}{CBR} - 17.8A} \qquad \textit{Eq.3}$$

Giroud and Noiray (1981) proposed another empirical formula for unreinforced unpaved road with rutting criteria (r) other than 75 mm:

$$h = \frac{(0.190 logN + 0.445(r - 0.075))}{CBR^{0.63}} \qquad \textit{Eq.4}$$

Where, H and r in meter; N = passages number of standard axle load 80 kN. This method is not recommended for N higher than 10,000 cycles or less than 20 cycles.

More recently, the analytical methods where developed to determine the aggregate thickness for reinforced unpaved roads on soft subgrade. Giroud and Han (2004) proposed the following :

$$H = \frac{\left(0.868 + \left(0.661 - 1.006.J_{ASM}^2\right)\right).\left(\frac{a}{h}\right)^{1.5}.\log N}{1 - 0.204.(R_E - 1)} . \left(\sqrt{\frac{\frac{P}{\pi r^2}}{\left(\frac{r}{fs}\right).\left(1 - 0.9e^{\left(-\left(\frac{a}{h}\right)^2\right)}\right).N_C.c_u}} - 1\right).r \qquad \textit{Eq.5}$$

$$c_u = f_c\, CBR_{sg} \qquad \textit{Eq.6}$$

$$R_E = \min\left(\frac{E_{bc}}{E_{sg}}, 5\right) = \min\left(\frac{3.48CBR_{bc}^{0.3}}{CBR_{sg}}, 5\right) \qquad \textit{Eq.7}$$

Leng and Gabr (2006) developed the following analytical solution to calculate the aggregate thickness:

$$H = \frac{(1+\left(\left(\frac{a}{h}\right)^{0.81}(0.58-0.000046J_t^{4.5})\right).\log N)}{\tan\alpha_1} . \left(\sqrt{\frac{p_c}{\left(\frac{r}{r_{cr}}\right).\left(1-e^{\left(-0.78\frac{a}{h}\right)}\right).N_C.c_u}} - 1\right).a \qquad Eq.8$$

These empirical and analytical methods were used to design such structure in the case of an unreinforced platform. For the empirical method (Hammitt and Iii, 1970), the CBR_{sg} was taken equal to 2%, the platform was designed to support 10,000 load passes of 40 kN, noting that the rutting criteria in this method is 75 mm. The same parameters were used for the empirical method of Giroud and Noiray (1981), while the N was taken equal 5,000 cycles, since in this method N is the passages number of standard axle load 80 kN.

Also for unreinforced case, the analytical method of Giroud and Han (2004) was used with the following parameters: Nc = 3.14; CBR_{sg}= 2 %; CBR_{bc}=12 %; P = 40 kN; pi = 560 kPa; N = 10,000 cycles; J_{ASM}= 0 mN/°; s =75 mm; fs = 75 mm. In addition, the analytical method of Leng and Gabr (2006) was used with the same parameters, only Nc is taken equal to 3.8 in unreinforced case, and J_t is taken equal to 0 kN/m.

The design of the reinforced platform with the previous analytical methods is not possible is this case. In fact, the geogrid type used in this work has a negligible aperture stability modulus J_{ASM} (mN/°). Moreover, this geogrid has an average geogrid tensile strength at 2% of strain of 20 kN/m, and in the analytical method of Leng and Gabr (2006), the expression involving the geogrid characteristics is negative for J_t > 8 kN/m. Therefore, the comparison with the empirical and analytical methods was done only for unreinforced conditions.

Table 6 resumes the design results of the empirical and analytical methods. Moreover, the designed base course thicknesses were compared to the experimental base course thickness taken equal to 350 mm, since the experimental surface rutting after 10,000 cycles is equal to 44 mm smaller than the rutting criteria of 75 mm.

As shown in Table 6, the empirical methods proposes a base course thickness of 460 mm without reinforcement, which is higher than the experimental base course thickness for about 30%.

The highest required thickness is given by Leng and Gabr (2006) and it over estimates the thickness of about 40%, regarding the proposed experimental base course thickness. It is evident that the procedure proposed by Leng and Gabr (2006) is more conservative comparing to the procedure of Giroud and Han (2004). In fact, the design dimension proposed by Giroud and Han (2004) is the lowest value and the closest one to the experimental proposed thickness. However, these conclusions are limited to the unreinforced platforms and to the experimental conditions taken in this work.

11. CONCLUSIONS

This paper presents an experimental study on the unpaved roads over soft subgrade. The aim of this experimental protocol is to characterise the influence of GSY reinforcement in this application. In this paper, we presented the first tests performed in order to validate the installation and preparation protocol, and verify the test repeatability. This validation tests were performed in order to prepare for further tests with different GSY types and positions. Moreover, circulation tests will be performed with the simulator accelerator of traffic developed at INSA Lyon especially for this application.

This experimental protocol allowed the subgrade and the base course settlement, the GSY deformation and the vertical stress distribution on the subgrade monitoring.

The unpaved road platform was subjected to cyclic plate loading. The surface rutting, the subgrade settlement and the stress distribution were monitored during tests. A special attention was given to the layer installation and the quality control, in order to reconstruct the same soil properties for every tests and insure a good repeatability.

Two tests were performed with the same configurations to check the repeatability, the measures of stress and vertical displacements validated this repeatability.

The reinforced and unreinforced tests performed on a thin (220 mm) and thick (350 mm) platforms show that the reinforcement has a negligible effect for thick platforms.

The comparison between a reinforced and unreinforced thin platform (220 mm), proves the efficiency of the reinforcement in rut development reduction. Indeed, for monotonic loading, the base course rut is decreased of 22% with reinforcement. The reinforcement decreases the central vertical stress at the interface subgrade/base course of about 17%. In addition, for cyclic loading, the GSY benefit was highlighted with the TBR ratio calculated for three different rutting: $TBR_{45mm} = 2$, $TBR_{60mm} = 7.5$ and $TBR_{75\ mm} = 24.3$. This shows that the reinforcement benefit is more important for high allowable rutting criteria.

It is worth it to point out that those results are limited to the geogrid type used in this study; future works will allow testing and comparing different geogrid types.

The technology of the fibre optic sensors allowed the measurement of the developed strain in the GSY during the cycles. It shows that after 1,000 cycles, the developed tension in the GSY during the loading is equal 15% of its ultimate tensile strength. Moreover, it shows that the plastic strain is about 60% of the total deformation during the loading. More importantly, it shows that there are no influence of the borders anchorage of the GSY on the results.

Based on the comparison between the design method and the experimental base course thickness required, we conclude that the design methods provided in the literature overestimate the required base course thickness in the case of an unreinforced platform. Moreover, the analytical design method proposed by Leng and Gabr (2006) is more conservative than the method proposed by Giroud and Han (2004) for the unreinforced case. However, these design methods could not be used with this specific GSY product to estimate the reinforced base course thickness.

12. ACKNOWLEDGMENTS

This study was performed in the framework of the new French Laboratory of Technical Innovations applied to Reinforcement GSYs (PITAGOR) funded in December 2015 by the French National Research Agency. The authors would like to thank the French National Research Agency that made this experimental study possible.

13. LIST OF SYMBOLS

A	Tire contact area (m²)
a	Radius of the equivalent tire contact area (m)
C_u	Subgrade undrained cohesion (kPa)
CBR	California bearing Ratio
CBR_{sg}	California bearing ratio of the subgrade soil
CBR_{bc}	California bearing ratio of the base course soil
E_{bc}	Elastic modulus of the base course
E_{sg}	Elastic modulus of the subgrade
f_s	Factor equal 75 mm
f_c	Factor equal to 30 kPa
H	Base course thickness (m)
J_{ASM}	Aperture stability modulus of geogrid (mN/°)
J_t	Average geogrid tensile strength at 2% of strain (kN/m)
N	Passages number
Nc	Bearing capacity factor
$N_{reinforced}$	Number of load cycles for the reinforced base
$N_{unreinforced}$	Number of load cycles for the unreinforced base

P	Wheel load (kN)
p_c	Tire contact pressure (kPa)
r	Rutting criteria (m)
r_{cr}	Critical subgrade deformation (mm)
R_E	Limited modulus ratio
α_1	Initial stress distribution angle (°)

8. REFERENCES

AASHTO, 1993. AASHTO Guide For Design Of Pavement Structures,. In p. II-69.

Abu-Farsakh MY, Akond I, Chen Q, 2016. Evaluating the performance of geosynthetic-reinforced unpaved roads using plate load tests. International Journal of Pavement Engineering, 17(10):901-12.

Christopher BR, Perkins SW, 2008. Full scale testing of geogrids to evaluate junction strength requirements for reinforced roadway base design. InProceedings of the Fourth European Geosynthetics Conference, Edinburgh, United Kingdom, International Geosynthetics Society.

Collin JG, Kinney TC, Fu X, 1996. Full scale highway load test of flexible pavement systems with geogrid reinforced base courses. Geosynthetics International, 3(4):537-49.

Cook J, Dobie M, Blackman D, 2016. The development of APT methodology in the application and derivation of geosynthetic benefits in roadway design. In The Roles of Accelerated Pavement Testing in Pavement Sustainability, pp. 257-275.

Cuelho E, Perkins S, 2009. Field investigation of geosynthetics used for subgrade stabilization. Montana. Dept. of Transportation. Research Programs.

Cuelho E, Perkins S, Morris Z, 2014. Relative operational performance of geosynthetics used as subgrade stabilization. Montana. Dept. of Transportation. Research Programs.

Dong YL, Han J, Bai XH, 2010. Bearing capacities of geogrid-reinforced sand bases under static loading. InGround Improvement and Geosynthetics, pp. 275-281.

FHWA, 1998. Geosynthetic Design and Construction Guidelines. In p. 150.

Gabr M, 2001. Cyclic plate loading tests on geogrid reinforced roads. Research Rep. to Tensar Earth Technologies.

Giroud JP, Ah-Line C, Bonaparte R, 1984. Design of unpaved roads and trafficked areas with geogrids. InPolymer grid reinforcement, pp. 116-127.

Giroud JP, 2009. An assessment of the use of geogrids in unpaved roads and unpaved areas. InJubilee Symposium on Polymer Geogrid Reinforcement. Identifying the Direction of Future Research, ICE, London.

Giroud JP, Han J, 2004. Design method for geogrid-reinforced unpaved roads. II. Calibration and applications. Journal of Geotechnical and Geoenvironmental Engineering, 130(8):787-97.

Hammitt, George M., and W. Aspinall Iii, 1970. Thickness Requirements for Unsurfaced Roads and Airfields; Bare Base Support. No. Aewes-tr-s-70-5. Army engineer waterways experiment station Vicksburg miss.

Hufenus R, Rueegger R, Banjac R, Mayor P, Springman SM, Brönnimann R, 2006. Full-scale field tests on geosynthetic reinforced unpaved roads on soft subgrade. Geotextiles and Geomembranes, 1;24(1):21-37.

Jersey SR, Tingle JS, Norwood GJ, Kwon J, Wayne M, 2012. Full-scale evaluation of geogrid-reinforced thin flexible pavements. Transportation Research Record, 2310(1):61-71.

Kim WH, Edil TB, Benson CH, Tanyu BF, 2006. Deflection of prototype geosynthetic-reinforced working platforms over soft subgrade. Transportation research record, 1975(1):137-45.

Leng J, Gabr MA, 2006. Deformation–Resistance Model for Geogrid-Reinforced Unpaved Road. Transportation research record, 1975(1):146-54.

Milligan GW, Jewell RA, Houlsby GT, Burd HJ, 1989. A new approach to the design of unpaved roads-part 1. Ground Engineering, 22(3).

Norwood GJ, Tingle JS, 2014. Performance of Geogrid-Stabilized Flexible Pavements. US Army Engineer Research and Development Center, Geotechnical and Structures Laboratory.

Palmeira EM, Antunes LG, 2010. Large scale tests on geosynthetic reinforced unpaved roads subjected to surface maintenance. Geotextiles and Geomembranes, 1;28(6):547-58.

Perkins SW, Ismeik M, 1997. A Synthesis and Evaluation of Geosynthetic-Reinforced Base Layers in Flexible Pavements-Part I. Geosynthetics International, 4(6):549-604.

Qian Y, Han J, Pokharel SK, Parsons RL, 2012. Performance of triangular aperture geogrid-reinforced base courses over weak subgrade under cyclic loading. Journal of Materials in Civil Engineering, 27;25(8):1013-21.

Qian Y, Han J, Pokharel SK, Parsons RL, 2011. Stress analysis on triangular-aperture geogrid-reinforced bases over weak subgrade under cyclic loading: An experimental study. Transportation Research Record, 2204(1):83-91.

Satyal SR, Leshchinsky B, Han J, Neupane M, 2018. Use of cellular confinement for improved railway performance on soft subgrades. Geotextiles and Geomembranes, 1;46(2):190-205.

Sun X, Han J, Kwon J, Parsons RL, Wayne MH, 2015. Radial stresses and resilient deformations of geogrid-stabilized unpaved roads under cyclic plate loading tests. Geotextiles and Geomembranes, 1;43(5):440-9.

Watts GR, Blackman DI, Jenner CG, 2004. The performance of reinforced unpaved sub-bases subjected to trafficking.

Yang X, Han J, Pokharel SK, Manandhar C, Parsons RL, Leshchinsky D, Halahmi I, 2012. Accelerated pavement testing of unpaved roads with geocell-reinforced sand bases. Geotextiles and Geomembranes, 32:95-103.

Figure 1 - Test setup

656 **Figure 2 - Particles size distribution (20 % Kaolinite 80 % Sand mixture)**

657 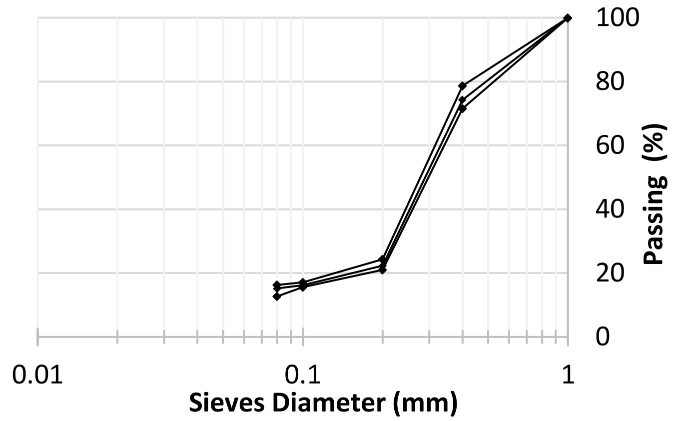

Figure 3 – 20 % Kaolinite 80 % Sand mixture Proctor and CBR curves

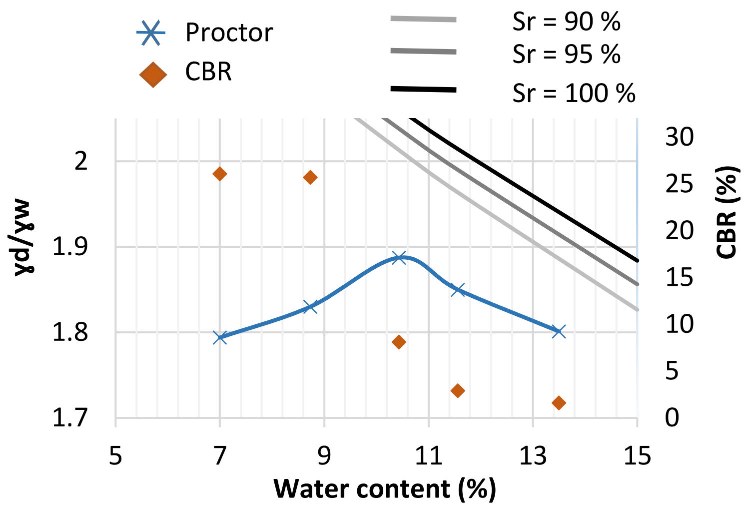

Figure 4 - Aggregates size distribution

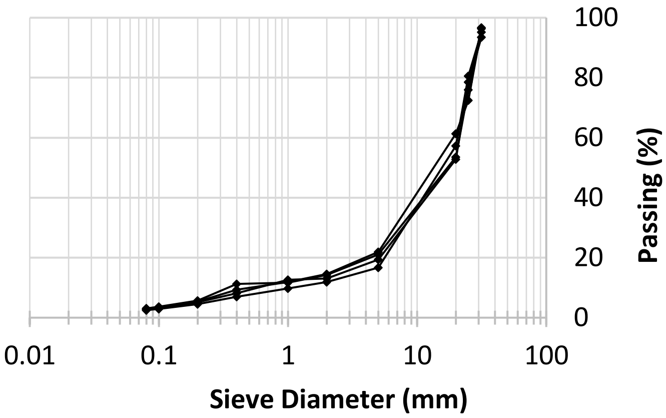

Figure 5 - Aggregates Proctor and CBR curves

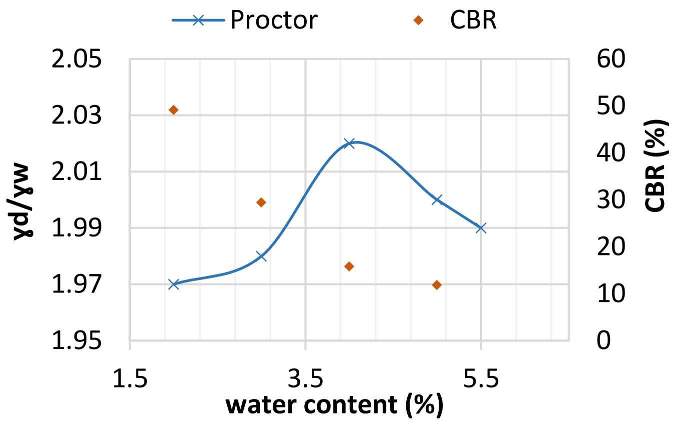

Figure 6 - The used GSY structure.

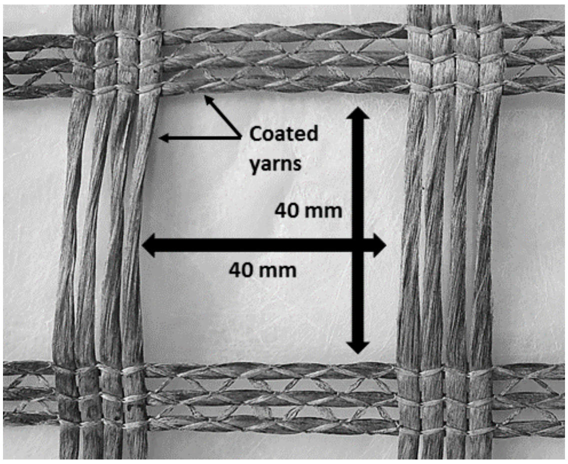

Figure 7 - The sensors installation plan

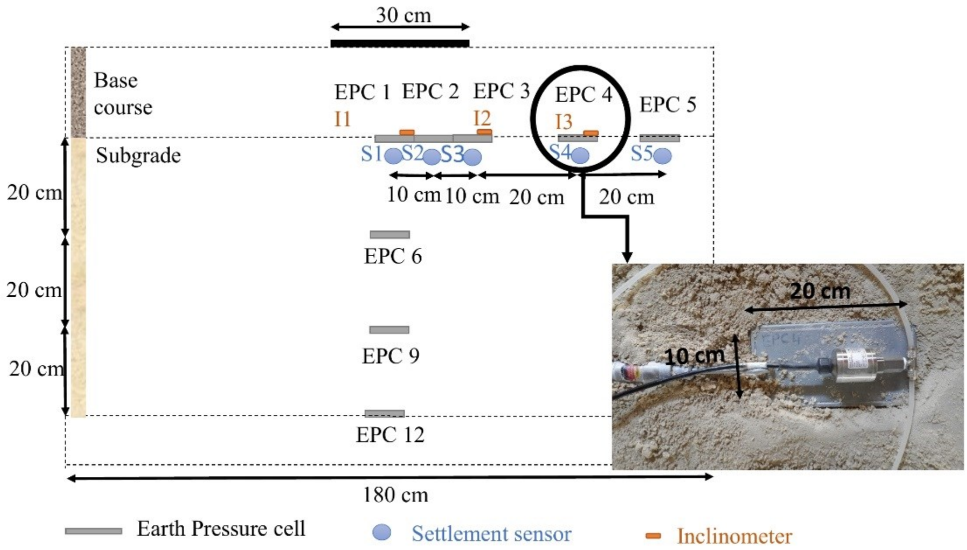

Figure 8 - the water content in depth for each prepared subgrade

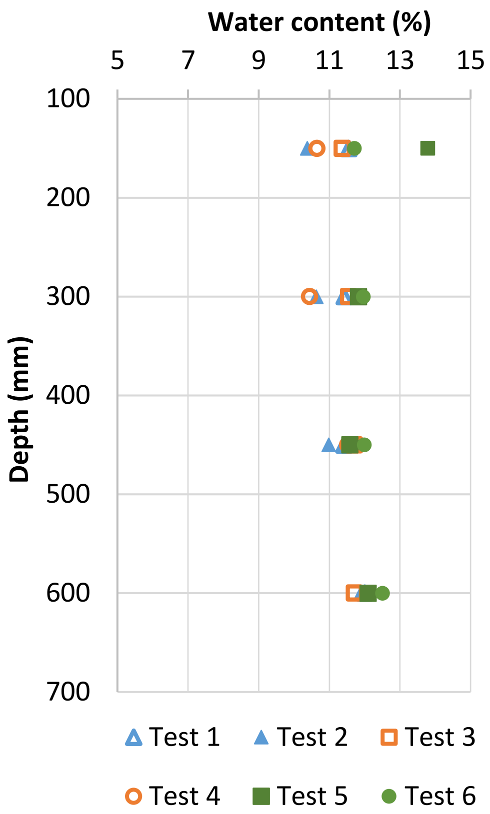

Figure 9 - CBR profile based on the dynamic penetrometer results correlation

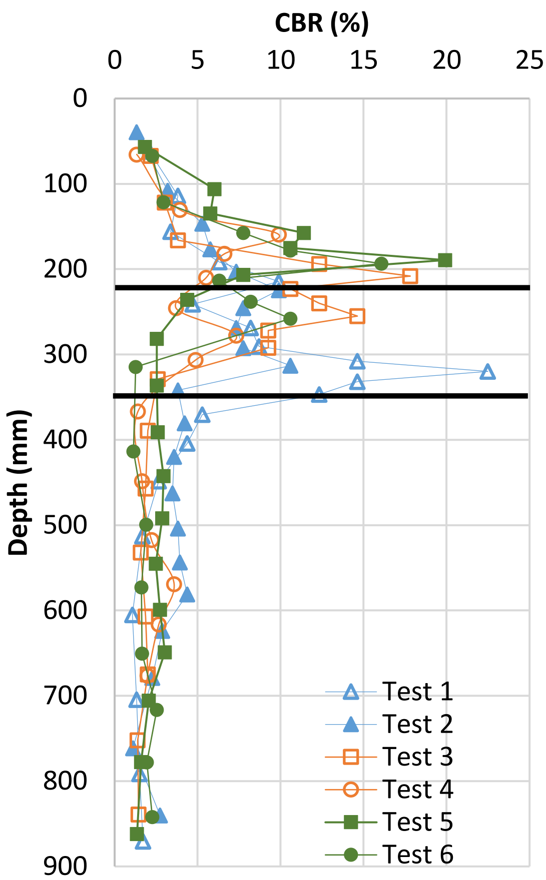

Figure 10 - Illustration of rut measurement

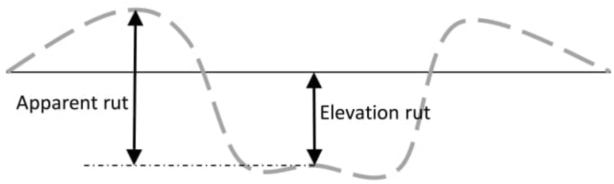

Figure 11 - Base course surface settlement after 10,000 cycles

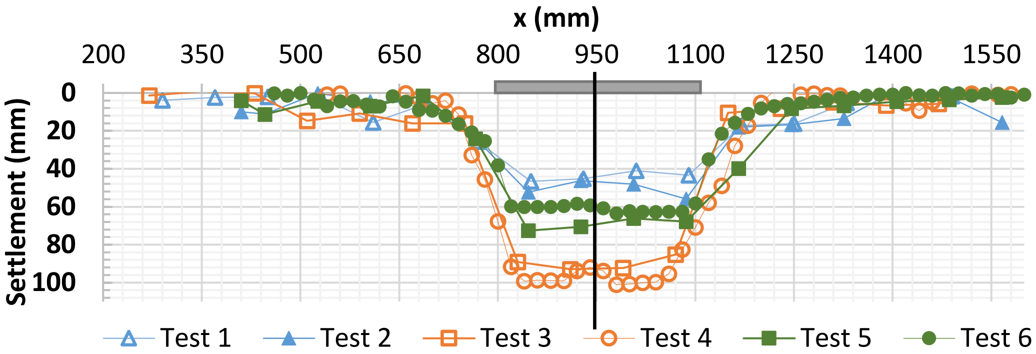

R: Reinforced platform U: Unreinforced platform
Test 1: U-350 mm Test 3: U-220 mm Test 5: R-220 mm
Test 2: R-350 mm Test 4: U-220 mm Test 6: U-220 mm

Figure 12 - Subgrade surface settlement evolution with the cycles, (a) after 500 cycles, (b) after 10,000 cycles

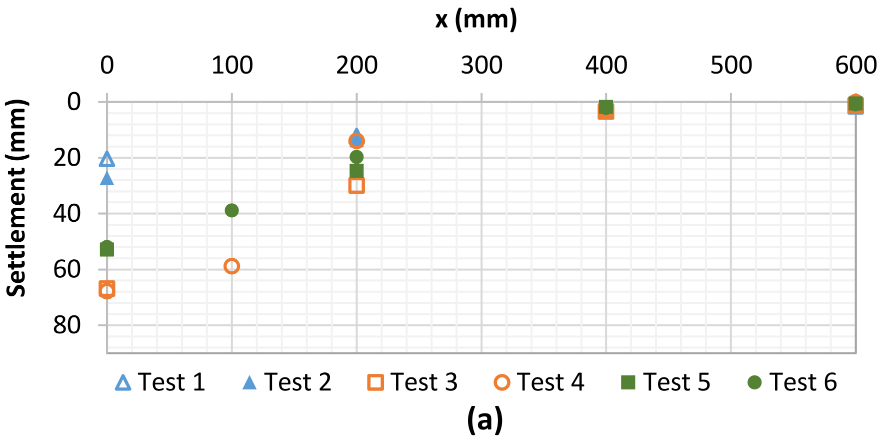

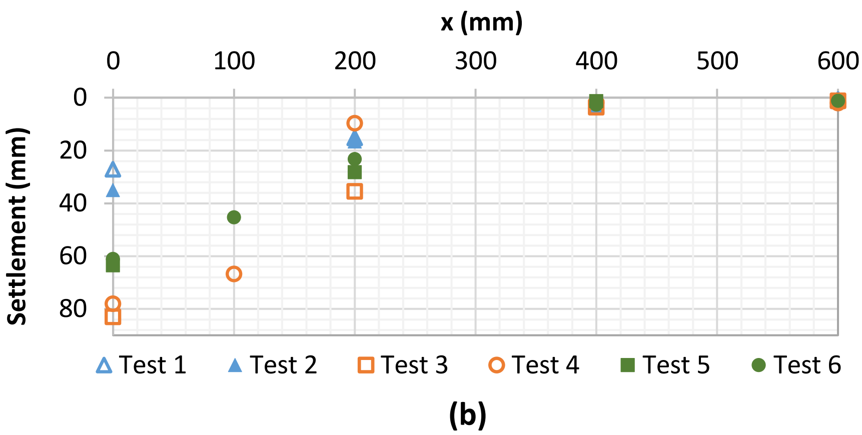

R: Reinforced platform U: Unreinforced platform
Test 1: U-350 mm Test 3: U-220 mm Test 5: R-220 mm
Test 2: R-350 mm Test 4: U-220 mm Test 6: U-220 mm

Figure 13 - Maximum settlement evolution with cycles at the centre of the subgrade surface for H = 220 mm

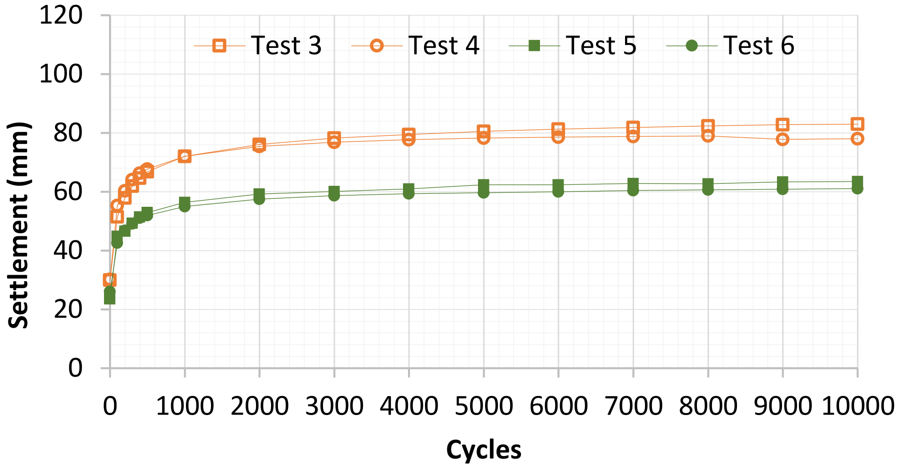

R: Reinforced platform U: Unreinforced platform
Test 3: U-220 mm Test 5: R-220 mm
Test 4: U-220 mm Test 6: U-220 mm

Figure 14 - Maximum settlement evolution with cycles at the centre of the base course for H = 220 mm

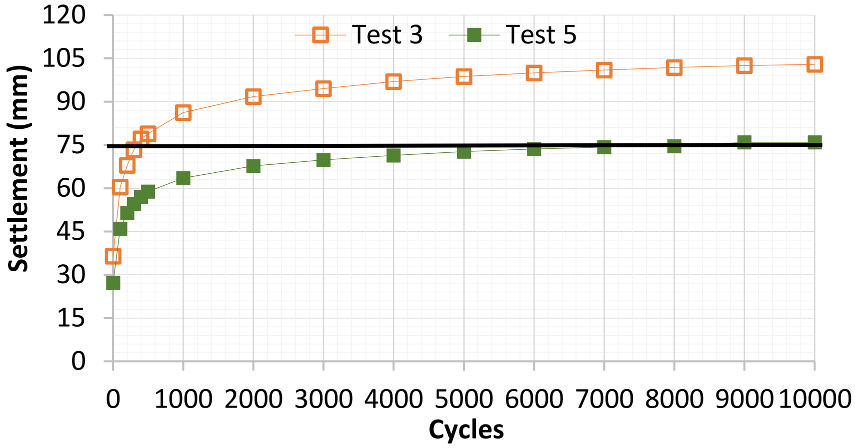

R: Reinforced platform U: Unreinforced platform
Test 3: U-220 mm Test 5: R-220 mm

686 **Figure 15 - Base course thickness reduction with cycles**

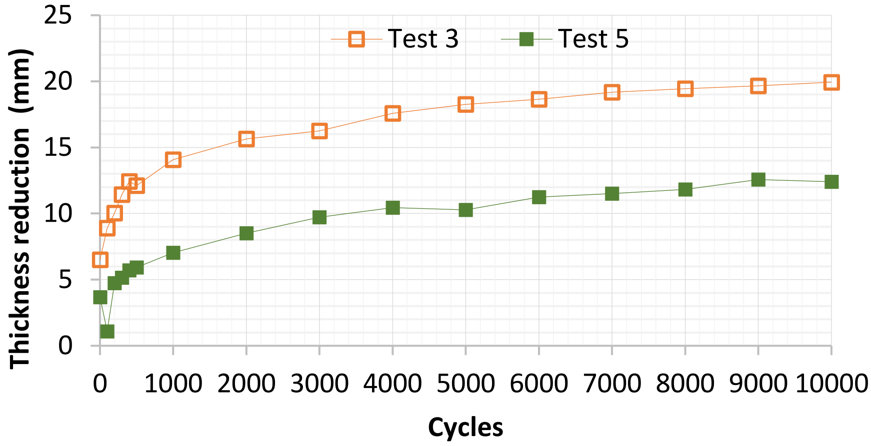

R: Reinforced platform U: Unreinforced platform
Test 3: U-220 mm Test 5: R-220 mm

687

Figure 16 - The vertical stress distribution at the subgrade surface, (a) after 500 cycles, (b) after 10,000 cycles

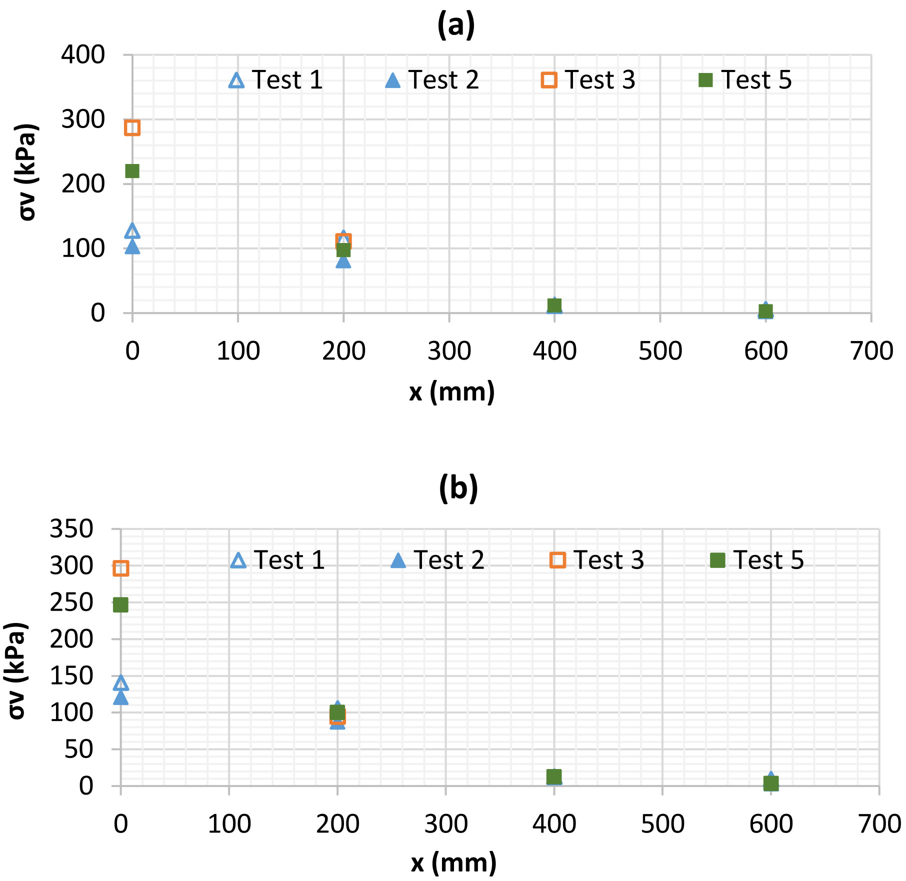

R: Reinforced platform U: Unreinforced platform
Test 1: U-350 mm Test 3: U-220 mm
Test 2: R-350 mm Test 5: R-220 mm

693 **Figure 17 - Vertical stress distribution along the subgrade depth**

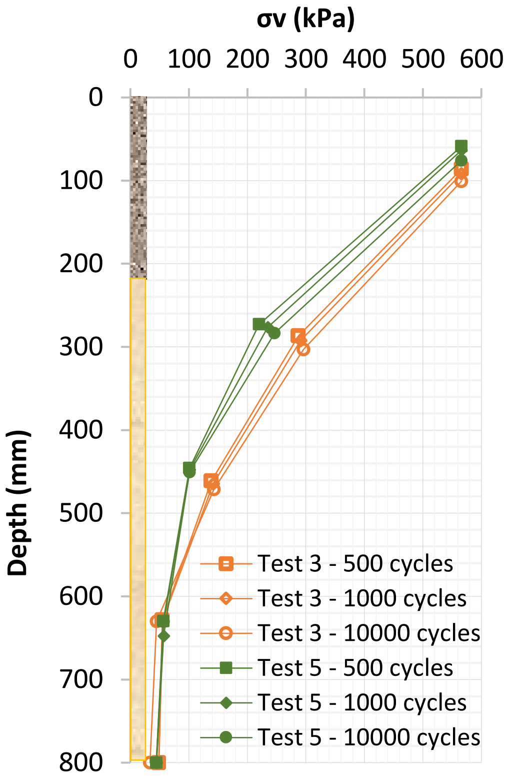

R: Reinforced platform U: Unreinforced platform
Test 3: U-220 mm Test 5: R-220 mm

694

Figure 18 - Maximum vertical stress at subgrade surface for specific base course settlement (45-60-75 mm) for H = 220 mm

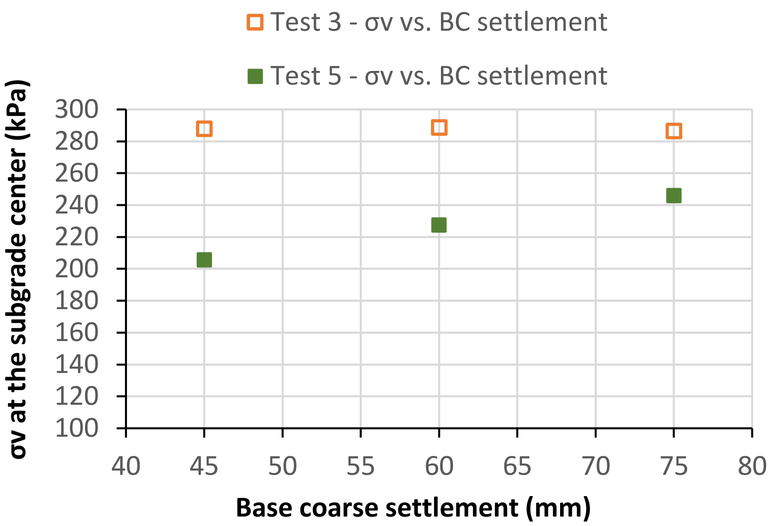

R: Reinforced platform   U: Unreinforced platform
Test 3: U-220 mm   Test 5: R-220 mm

Figure 19 - The Strain/Force developed in the GSY during installation

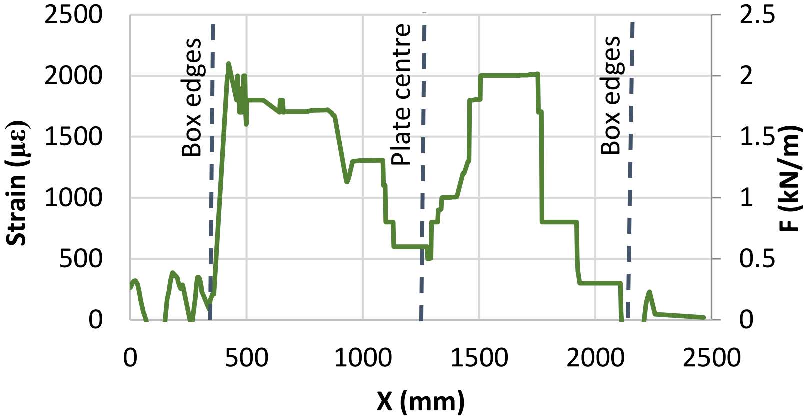

Figure 20 - The Strain/Force developed in the GSY after 1,000 cycles, during the loading and unloading

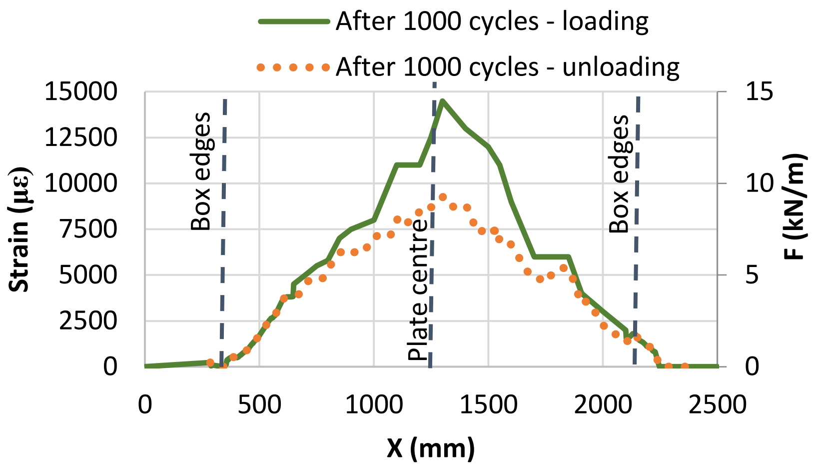

Table 1 – Degree of saturation measured for 4 mixtures

Mixture	20 % Clay 80 % Sand	25 % Clay 75 % Sand	30 % Clay 70 % Sand	40 % Clay 60 % Sand
Kaolinite	$Sr_{(CBR\ 2\ \%)} = 75\ \%$	$Sr_{(CBR\ 2\ \%)} = 80\ \%$	$Sr_{(CBR\ 2\ \%)} = 90\ \%$	$Sr_{(CBR\ 2\ \%)} = 95\ \%$
Calcium Bentonite	---	$Sr_{(CBR\ 2\ \%)} = 90\ \%$	$Sr_{(CBR\ 2\ \%)} = 95\ \%$	$Sr_{(CBR\ 2\ \%)} = 95\ \%$

Table 2 - Geogrid properties

Name	Type	Nature	Stiffness at 2 % (kN/m)	square Aperture (mm)	Maximum tensile strength (kN/m)	
					SP*	ST*
GSY 1	NotexC	PET	1,000	40	100	100

Table 3 - Used sensors properties

	Type	Size	Range
Earth Pressure Cells	Electrical pressure cell	100 x 200 mm	0-500 kPa
Settlement sensors	Hydraulic settlement sensor	Φ 50 x 62 mm	0-300 mm
Displacement sensor	Laser sensor	--	0-200 mm

Table 4 - Tests details

Test number	Base course thickness (mm)	Reinforcement	Test status
Test 1	350	Without reinforcement	Reference test
Test 2	350	GSY	GSY improvement test
Test 3	220	Without reinforcement	Reference test
Test 4	220	Without reinforcement	Repeatability test
Test 5	220	GSY	GSY improvement test
Test 6	220	GSY	Repeatability test

Table 5 – Number of Cycles and TBR for specific base course settlement for H = 220 mm

Base course Settlement (mm)	$N_{reinforced}$	$N_{unreinforced}$	TBR
45	100	50	2
60	750	100	7.5
75	8,500	350	24.28

Table 6 - Designed base course thicknesses estimation in the unreinforced case

The design methods	Designed base course thickness (mm)	Experimental base course thickness (mm)
Hammitt and Iii (1970)	460	< 350
Giroud and Noiray (1981)	460	
Giroud and Han (2004)	390	
Leng and Gabr (2006)	590	